

FastGL: A GPU-Efficient Framework for Accelerating Sampling-Based GNN Training at Large Scale

Zeyu Zhu^{1,2} Peisong Wang¹ Qinghao Hu¹ Gang Li³ Xiaoyao Liang³ Jian Cheng^{1,2,4,5,†}

¹Institute of Automation, CAS

²School of Future Technology, University of Chinese Academy of Sciences

³Shanghai Jiao Tong University

⁴AiRiA ⁵Maicro.ai

{zhuzeyu2021, huqinghao2014}@ia.ac.cn, gliaca@sjtu.edu.cn, liang-xy@cs.sjtu.edu.cn

{peisong.wang, jcheng}@nlpr.ia.ac.cn

Abstract

Graph Neural Networks (GNNs) have shown great superiority on non-Euclidean graph data, achieving ground-breaking performance on various graph-related tasks. As a practical solution to train GNN on large graphs with billions of nodes and edges, the sampling-based training is widely adopted by existing training frameworks. However, through an in-depth analysis, we observe that the efficiency of existing sampling-based training frameworks is still limited due to the key bottlenecks lying in all three phases of sampling-based training, i.e., subgraph sample, memory IO, and computation. To this end, we propose **FastGL**, a GPU-efficient Framework for accelerating sampling-based training of GNN at Large scale by simultaneously optimizing all above three phases, taking into account both GPU characteristics and graph structure. Specifically, by exploiting the inherent overlap within graph structures, FastGL develops the **Match-Reorder** strategy to reduce the data traffic, which accelerates the memory IO without incurring any GPU memory overhead. Additionally, FastGL leverages a **Memory-Aware** computation method, harnessing the GPU memory’s hierarchical nature to mitigate irregular data access during computation. FastGL further incorporates the **Fused-Map** approach aimed at diminishing the synchronization overhead during sampling. Extensive experiments demonstrate that FastGL can achieve an average speedup of 11.8 \times , 2.2 \times and 1.5 \times over the state-of-the-art frameworks PyG, DGL, and GNNLab, respectively. Our code is available at <https://github.com/a1bc2def6g/fastgl-ae>.

1 Introduction

Recently, Graph Neural Networks (GNNs) have attracted much attention from both industry and academia due to their superior learning and representing ability for non-Euclidean graph data. A number of GNNs [12, 21, 34, 41] have been widely used in various graph-related tasks, such as social

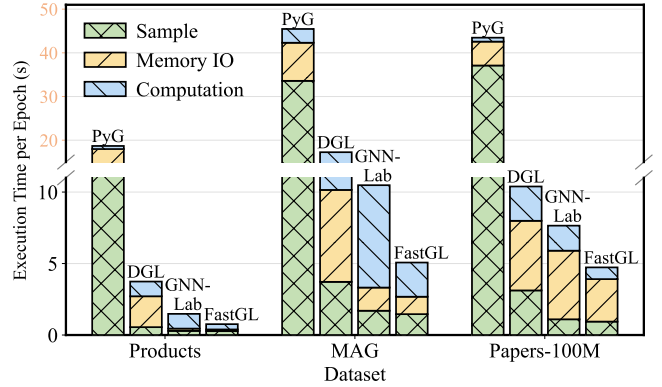


Figure 1. The execution time breakdown analysis of training GCN on various graphs using different sampling-based training frameworks. More experiment setup is detailed in Section 6.1.

network analysis [9, 23], autonomous driving [22, 40], and recommendation systems [18, 45].

In practice, many real-world graphs are large-scale and associated with rich node attributes (i.e., features). For example, the Pinterest graph [46] contains over 2 billion nodes and 17 billion edges with 18TB data size. Such a large size makes it impossible to load the entire graph into the GPU with only tens of gigabytes memory, which turns down proposals designed for full-graph training on GPUs [17, 35]. A practical solution to this problem is the sampling-based GNN training [12, 15, 46], which adopts a sampling algorithm to extract subgraphs from the entire graph and trains GNNs on these sampled subgraphs.

For the sampling-based GNN training frameworks [10, 25, 26, 38, 43, 50], the CPU host memory is used to store graphs including graph topology information and nodes features, and GPUs are responsible for model training. Each iteration of the sampling-based training consists of three stages: (1) *sample* subgraphs and store them in host memory, (2) load structures of subgraphs and features of sampled nodes to GPUs (referred to as *memory IO* phase), (3) launch the forward and backward *computations* for GNN training. While the sampling-based training is ingenious, it comes with a significant drawback - the high overhead of data traffic and

[†]Corresponding author.

*This is the author’s version of the work. It is posted here for personal use. Not for redistribution. The definitive Version of Record was published in 29th ACM International Conference on Architectural Support for Programming Languages and Operating Systems, Volume 4 (ASPLOS ’24), April 27-May 1, 2024, La Jolla, CA, USA, <http://dx.doi.org/10.1145/3622781.3674167>

sampling. This is due to the large number of mini-batches that need to be trained [10, 38], which seriously slows down the training process and hinders GNNs’ real-world applications on large-scale graphs. Although a spectrum of frameworks [10, 25, 26, 38, 43, 49, 50] have been proposed to expedite this process, through our in-depth analyses in Figure 1, we observe that they still cannot unlock the acceleration potential due to the following three performance bottlenecks:

Insufficient support for fast sampling. First, existing frameworks often perform graph sampling on the CPU, which is extremely time-consuming due to the poor parallelism. For example, PyG [10] spends up to 97% of the overall training time to sample on CPU. Second, in the sample phase, the global ID of each sampled node in the raw graph needs to be converted to a local ID in the sampled graph (this process is referred to as *ID map*) to avoid loading all nodes features to the GPU memory. Although DGL [38] utilizes the thread parallelism of GPU to accelerate the sample phase, the vast volume of thread synchronizations to obtain the local IDs still incurs considerable latency overhead into the sample phase, which occupies up to 38% time.

Failing to accelerate the memory IO on large-scale graphs. Since the bandwidth between host memory and GPU memory is low (e.g., 32GB/s of PCIe 4.0 with 16 channels), the memory IO phase dominates the overall training time (up to 77%) and significantly impedes performance boosting. This phenomenon is exacerbated as the graph size increases. PaGraph [25] and GNNLab [43] both regard a portion of GPU memory as a software-controlled cache to reduce the data traffic between the CPU and GPU. However, the device memory in GPU is a scarce resource and there is little or no extra memory to be used as a cache especially in the large-scale graph scenario, which makes these methods inefficient.

Irregular memory access during the computation. For real-world graphs, the connections are extremely sparse and unstructured [12, 13, 24], and hence inducing great irregularity into the computation phase when accessing data (e.g., features and edge weights) according to edges. The irregularity results in poor hit rates (4.41%/19.6% on average) of the L1/L2 cache on GPU, which seriously limits the bandwidth available to the computing units, thereby hampering the GPU performance and decelerating the computation. Previous works overlook optimizations on memory accesses, making the computation phase another bottleneck.

To tackle the above challenges, we focus on accelerating all phases of the sampling-based GNN training in this paper by taking into account both GPU characteristics and graph structure under the single machine with multiple GPUs scenario. For the biggest bottleneck (except in PyG), i.e., memory IO, we first reveal that there are great overlap across different sampled subgraphs, stemming from the complex graph structures. This motivates us to design a greedy strategy of **Match-Reorder** to maximally reuse the overlapping nodes between mini-batches, which reduces the magnitude of data

traffic between CPU and GPU without imposing any GPU memory cost. Furthermore, to mitigate the irregularity in the computation, we introduce the **Memory-Aware** computation approach that capitalizes on the disparities in bandwidth across different GPU memory levels. By adjusting the memory access pattern, we enhance the overall bandwidth utilization and GPU performance, consequently speeding up the computation phase. Finally, we develop the **Fused-Map** sampling method to fuse the necessary operations in the ID map process, thereby significantly reducing the volume of thread synchronizations and expediting the sample phase.

We integrate the above design ideas into **FastGL**, a GPU-efficient Framework tailored for accelerating sampling-based training of GNN on Large-scale graphs, which substantially accelerates the sampling-based GNN training.

In summary, the contributions of this paper are as follows:

- We conduct a breakdown analysis of the sampling-based GNN training on large-scale graphs and identify three main performance bottlenecks. To mitigate the biggest bottleneck, i.e., memory IO, we propose the **Match-Reorder** strategy to maximally reduce the data traffic without inducing any GPU memory overhead.
- To accelerate the computation phase, we put forward the **Memory-Aware** computation approach, which redesigns the memory access pattern to increase the GPU performance by exploiting different levels of memory in GPU.
- We propose the **Fused-Map** sampling method to avoid the thread synchronizations and expedite the sample phase by performing the ID map process in a fused mechanism.
- We implement the proposed framework **FastGL** equipped with the above three techniques and conduct extensive experiments with various GNN models and large-scale graph datasets. On average, FastGL can improve the training efficiency by 11.8×, 2.2× and 1.5× over the state-of-the-art PyG [10], DGL [38], and GNNLab [43], respectively.

2 Background and Related Work

2.1 Graph Neural Networks.

Graph Neural Networks (GNNs) [12, 21, 34, 41] are deep learning models aiming at addressing graph-related tasks in an end-to-end manner. Given a graph $G = (V, E)$, which consists of $|E|$ edges and $|V|$ nodes, and each node is associated with a feature vector. In each GNN layer, the forward pass contains two phases: the aggregation and the update. In the aggregation phase, the target node u collects weighted information from its neighbors (referred to as source nodes) following the graph structure and generates the hidden features as follows:

$$\mathbf{h}_u^{k+1} = \sum_{v \in N(u)} w_{uv}^k \cdot \mathbf{x}_v^k, \quad (1)$$

where k denotes the k -th layer of GNN, $N(u)$ represents the neighbors of the node u , $\mathbf{x}_v \in \mathbb{R}^d$ is the feature vector of node v , $w_{uv} \in \mathbb{R}$ is the weight and \mathbf{h}_u is the aggregated hidden features of node u . Then, the hidden features of each node are

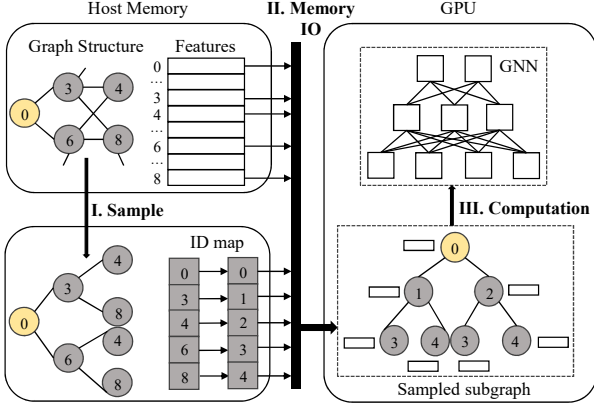


Figure 2. An example of the sampling-based training in a 2-layer GNN on the training node 0. The sampling algorithm uniformly selects two neighbors for each node.

transformed to the new features as the output of the current layer in the update phase as follows:

$$\mathbf{x}_u^{k+1} = \text{Update}^{k+1}(\mathbf{h}_u). \quad (2)$$

A GNN model learns a low-dimensional embedding for each node by recursively performing the above process, which would be used in various downstream tasks [9, 12, 21].

2.2 Sampling-based GNN Training.

There are two categories of training paradigms adopted in existing GNN systems: full-batch training and sampling-based training. Full-batch training loads the entire graph into GPUs for training [21], such as NeuGraph [27], ROC [17], and FlexGraph [37]. Unfortunately, for large-scale graphs, such an approach is limited by the GPU memory capacity. Therefore, we focus on the sampling-based training in this paper.

The sampling-based approach (also referred to as mini-batch training) [4, 12, 15, 47] splits the training nodes into multiple mini-batches and samples the subgraphs according to these mini-batches and then conducts GNN training on subgraphs iteratively. Training on one mini-batch is called an iteration, which consists of three phases as shown in Figure 2, i.e., **sample**, **memory IO** and **computation**. In general, the sample phase is divided into two steps. (1) **sample subgraph**: Starting from each node in a mini-batch, the input subgraph is sampled according to a user-defined sample algorithm. (2) **ID map**: To update the subgraph structure, the global ID of each sampled node in the raw graph needs to be converted to a local ID (consecutive and start from 0) in the sampled graph. After sampling, the features of sampled nodes and subgraph structures are loaded from host memory to GPU memory. Finally, GPU launches the computation for GNN training on the sampled subgraph.

2.3 GNN Training Frameworks.

In recent years, two categories of GNN training frameworks are also developed upon existing deep learning frameworks for efficient GNN training, i.e., full-batch training framework

[17, 27, 32, 35–37] and sampling-based training framework [10, 11, 14, 38, 42, 44, 50]. Constrained by GPU memory, full-batch training frameworks cannot scale efficiently to large-scale graphs, thus we focus on the presentation of sampling-based training frameworks in this section.

PyG [10] integrates with PyTorch [29] to provide a message-passing API for GNN training. However, sampling by CPUs, PyG cannot scale well to large graphs. DGL [38] accelerates the sample process by utilizing GPUs, which has much higher parallelism than CPUs. However, the enormous thread synchronizations on GPUs incur heavy latency overhead to the sample. And the vast volume of data traffic between host memory and GPU memory further limits the training efficiency. Much worse, current frameworks [10, 38, 50] ignore the problem of poor cache hit rates caused by the extreme irregularity of the graph structure, which leads to the computation phase being another performance bottleneck.

To overcome the above problems, some more efficient sampling-based GNN training frameworks are proposed [2, 25, 26, 39, 43, 49]. PaGraph [25] and GNNLab [43] both regard a portion of GPU memory as a cache and propose the corresponding cache policy to reduce the data traffic between the CPU and GPU. However, GPU memory is a scarce resource, and there is often no extra space on the GPU to be used as a cache, especially when the sampled subgraphs are large. Dedicated for full-batch training, GNNAdvisor [39] preprocesses the graph according to its properties and proposes a 2D workload management to accelerate the computation. However, for the sampling-based training, the sampled subgraphs must be preprocessed in each iteration, incurring severe pre-processing overhead. There are also some works [16, 19, 28] that aim to accelerate the sample phase based on GPU or CPU. Unfortunately, sampling on CPUs [19] do not utilize GPU parallelism, and [16, 28] overlook the latency overhead induced by the numerous thread synchronizations.

3 Motivation

3.1 Rethinking the Acceleration of Memory IO

To identify the bottleneck of the sampling-based GNN training, we conduct an execution time breakdown analysis of its three phases, i.e., sample, memory IO, and computation on Products dataset of GCN [21] and GIN [41] model, as depicted in Figure 3. ‘Naive’ denotes that the time is obtained by running the model with DGL [38]. We observe that by consuming up to 77% of the training time, the memory IO dominates the overall training process. This is primarily due to the vast volume of data transferred from host memory to GPU memory, a challenge further compounded in large-scale graphs by the limited bandwidth (e.g., 32GB/s of PCIe 4.0 with 16 channels).

Many existing works focus on resolving the bottleneck of memory IO [25, 26, 31, 43], whose key idea is to regard a portion of GPU memory as a software-controlled cache,

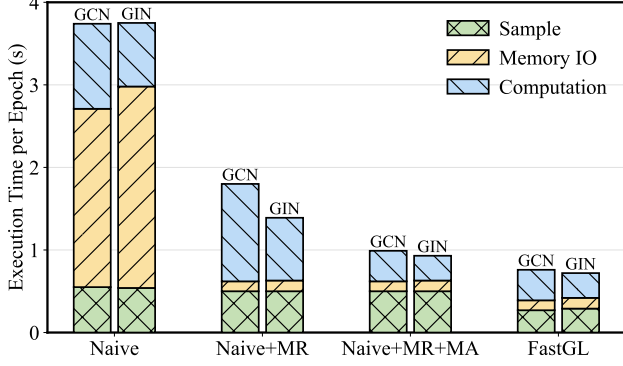


Figure 3. The execution time breakdown analysis on Products dataset of GCN and GIN on two NVIDIA RTX 3090 GPUs. The average time is generated from 20 epochs.

Table 1. The remaining GPU memory when running a 3-layer GCN on different graphs based on DGL. Measured on one 3090 GPU with 24GB memory, the batch size is 8000, and the hidden size is 256.

Graph	Reddit	Products	MAG	Papers-100M
Left Memory	13GB	11GB	520MB	1GB

and perform various optimizations on the cache policy to cache nodes features more efficiently. Upon cache hit, the data traffic between CPU and GPU can be saved. However, as presented in Table 1, the GPU memory is a scarce resource and there is little or no left memory to be used as a cache because the sampled subgraphs are large, which is caused by the neighbor explosion problem [5, 47]. In such a scenario, the previous works can only cache a small (even no) fraction of nodes features on GPU due to the memory constraints and they are no longer effective in reducing data traffic. For example, the hit rate of PaGraph is less than 20% on MAG. Although naively reducing the mini-batch size leaves more GPU memory available, this proportionally increases the number of mini-batches to be trained, which significantly offsets the benefits gained from memory I/O optimization.

Thanks to the complex topology in the large-scale graph, i.e., one node often connects with multiple nodes and may be sampled in different subgraphs, there is a high degree of node overlap (up to 96%) between different subgraphs. This motivates us to propose the Match-Reorder (MR) strategy where Match reduces the data traffic by reusing the overlapping nodes without imposing any GPU memory cost and Reorder maximizes the reuse.

3.2 Opportunity in the Computation Acceleration

As shown in Figure 3 (‘Naive+MR’), after optimizing the memory IO, the computation phase renders the primary performance bottleneck due to the the great irregularity of memory

Table 2. The hit rates of L1/L2 cache and the achievable performance of 3090 GPU in the forward process of the aggregation phase.

Graph	Reddit	Products	MAG	Papers-100M
L1 Cache	3.34%	5.11%	4.92%	4.25%
L2 Cache	24.6%	18.3%	15.7%	19.6%
GFLOP/s	340	397	380	401

* Measured by the NVIDIA Nsight Compute 2023.1.

Table 3. The statistics of different memory levels in 3090 GPU.

	L1 Cache	Shared Memory	L2 Cache	Global Memory
Bandwidth	~12TB/s	~12TB/s	3~5TB/s	938GB/s
Capacity	128KB (per SM)		6MB	24GB

accesses induced by the extremely sparse connections between nodes during the aggregation. Table 2 presents the L1/L2 cache hit rate and the achievable GPU performance during the aggregation phase. The low hit rate limits the bandwidth attainable to the computing units and results in the achievable GPU performance being much lower than the theoretical peak performance (29155GFLOP/s of 3090 GPU), incurring severe latency overhead into the computation.

Fortunately, in addition to the L1/L2 cache, there are multiple memory levels on GPU with widely varying bandwidth, as shown in Table 3. Intuitively, the more data is stored in the memory with a higher bandwidth, the higher overall bandwidth is available to the computing units. However, limited by the memory capacity, only a fraction of data can be stored in the higher bandwidth memory. Accordingly, we first analyze the memory access pattern in the aggregation and then propose the Memory-Aware (MA) method, which prioritizes the storage of frequently accessed data in higher-bandwidth memory to increase the overall bandwidth and accelerate the computation phase.

3.3 Bottleneck Existing in the Sample Phase

Our breakdown analysis in Figure 3 (‘Naive+MR+MA’) indicates that the sample phase now impedes the performance boosting with the two above optimizations, which costs more than 50% time of the overall training process. Through a further analysis, we observe that the ID map process takes up to 70% time of the sample phase. As detailed in Figure 4b-d, the ID map comprises three steps: (1) construct a hash table for fast global ID indexing, (2) obtain the local ID and record the map between global ID and local ID, and (3) transform global IDs to local IDs using the hash table.

DGL [38] accelerates step (1) and (3) by leveraging GPU’s massive threads parallelism, assigning each thread to a single global ID. However, the concurrent computation of local IDs

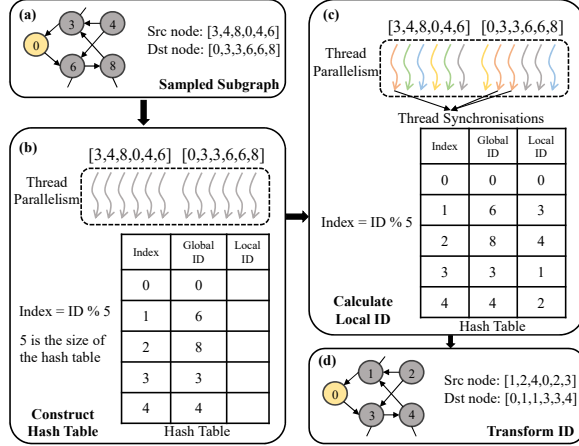


Figure 4. Illustration of the ID map process.

in stage (2) necessitates synchronization to prevent multiple threads from repeatedly accumulating for the same global ID, which would lead to conflicting mappings. For example, without synchronizations, the threads processing the global ID 3 will accumulate three times, resulting in the global ID 3 corresponding to multiple local IDs. The extensive thread synchronizations considerably slow down the ID map.

To alleviate this problem, we propose the Fused-Map sampling approach to perform the ID map process in a fused mechanism, which avoids the numerous thread synchronizations and expedites the sample phase (‘FastGL’ of Figure 3).

4 Design

In this section, we present the **FastGL** framework equipped with our three proposed innovative techniques, which tackles the above bottlenecks well and substantially unlocks the acceleration potential of GNN training on GPU.

Figure 5 shows the overall architecture of our FastGL framework. From the start of each epoch, the Map-Fused Sampler samples n mini-batches. Then FastGL reorders the computation order of the n mini-batches with the Reorder strategy. Once the reorder is done, the data of the first mini-batch are loaded to GPU to participate in the forward and backward computations, which would be accelerated by our Memory-Aware computation method. After completing the training of the current mini-batch, FastGL loads the nodes features required by the next mini-batch through our Match process to accelerate the memory IO phase. We repeat the above process for the next n mini-batches until finishing an epoch. M GPUs complete the training in a data parallel manner.

4.1 Match-Reorder Strategy

Previous works [25, 43] incur heavy GPU memory overhead when optimizing the memory IO, which is infeasible for large-scale graphs. This calls for a more efficient design that reduces the data traffic without requiring any extra GPU memory.

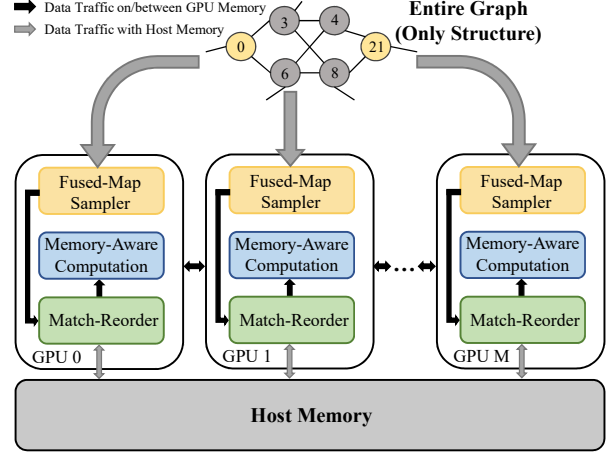


Figure 5. Overall architecture of FastGL.

Table 4. The average match degree and the differences in match degrees between mini-batches on different graphs. ΔM denotes the difference between the maximum and minimum M_{ij} in one epoch.

Graph	Reddit	Products	MAG	Papers-100M
$Avg(M_{ij})$	93.2%	71.4%	35.3%	38.0%
ΔM	4.9%	7.0%	4.2%	5.3%

* Batch size is 8000 with uniform sampling.

Jangda et. al. proposed NextDoor [16] and qualitatively revealed that the same node may appear in different sampled subgraphs. Our in-depth quantitative analysis further demonstrates that there is a large number of overlapping nodes between different sampled subgraphs thanks to the complex topology of a graph. M_{ij} is the *match degree* to represent the ratio of overlapping nodes between subgraph i and subgraph j , i.e., $M_{ij} = \frac{N_o}{\min(N_i, N_j)}$, where N_o is the number of overlapping nodes and N_i/N_j is the total number of the nodes in subgraph i/j . Table 4 presents the average *match degree* in one epoch on different graphs, which could be up to 93.2%.

Therefore, we propose the **Match** method, which performs the match before loading the nodes features of a new mini-batch except the first one to reuse the features of overlapping nodes. We first calculate the intersection (denoted as *OverlapNodeID*) of the nodes in the mini-batch to be computed on GPU and the nodes of the last mini-batch. Then we obtain the global IDs of the nodes required to be loaded from the host memory to GPU memory (*LoadNodeID*) through subtracting *OverlapNodeID* from the node sets of the mini-batch to be computed. GPU only loads the features of the nodes whose IDs are in the *LoadNodeID*. The **Match** process reduces the data traffic by reusing and does not require any extra consumption of GPU memory because the memory occupied by the last mini-batch is necessary. As an example shown in Figure 6(a), when finishing the training of the first

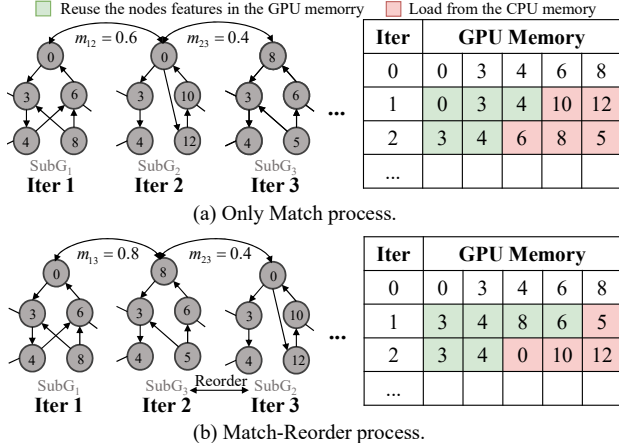


Figure 6. An example of our Match-Reorder method. m_{ij} denotes the match degree between the subgraph i and j .

Algorithm 1 Greedy Reorder Strategy

```

1: Initialize:  $NodeIDList = \{NodeID_1, NodeID_2, \dots, NodeID_n\}$ ,
    $NodeID_i$  is the node IDs in the  $i$ -th mini-batch;  $ReorderedList$ :
   the list to store the reordered mini-batches.
2: Greedy Reorder ( $n$ ):
3: Calculate the match degree matrix  $M$ ,  $m_{ij}$  is the match degree
   between the  $i$ -th and the  $j$ -th mini-batches
4:  $ReorderedList.insert(SubG_1, 1)$ 
5:  $z = 1$  # the index of the last inserted mini-batch
6: for  $i = 2$  to  $n$  do
7:    $h = \arg \max_k m_{zk}$ 
8:    $ReorderedList.insert(SubG_h, i)$ 
9:   Set the  $z$ -th row and column of  $M$  to 0
10:   $z = h$ 
11: end for
12: return  $ReorderedList$ 
13: end

```

subgraph ($SubG_1$) in the 1-st iteration, GPU only loads the features of node 10 and 12 from CPU and reuses the features of the overlapping nodes, i.e., node 0, 3 and 4.

However, as the ΔM shown in Table 4, the *match degree* varies widely between different pairs of sampled subgraphs. Therefore, the computation order of the mini-batches would affect the reuse of the overlapping nodes, which may be sub-optimal under the default sample order.

To mitigate this problem, we propose the **Greedy Reorder Strategy** to maximize the reuse by reordering the computation order of the sampled mini-batches in a greedy manner. As shown in Algorithm 1, we first sample n mini-batches at a time and initialize the $NodeList$ using the global IDs of the nodes in each mini-batch (line 1). We then calculate the *match degrees* between the n subgraphs (line 3) and add the 1-st sampled subgraphs ($SubG_1$) into the $ReorderedList$ as the first mini-batch (line 4). Then, we search for the subgraph that has the maximum *match degree* with the subgraph last added into the $ReorderedList$ and insert this subgraph into the

$ReorderedList$ (line 7-8). To avoid inserting the same subgraph, we set the *match degrees* of subgraphs that have been inserted to zero (line 9). After conducting the above process for all n mini-batches, the $(i+1)$ -th mini-batch in the $ReorderedList$ has the maximum *match degree* with the mini-batch at the i -th location. By performing the computation as the order in the $ReorderedList$ and alternating the mini-batches with the **Match** process, we can significantly improve the reuse of the overlapping nodes. When these n mini-batches complete the training, we repeat the above process for the next n mini-batches until finishing one epoch.

As shown in Figure 6(b), after applying the Reorder strategy, the execution order of the $SubG_2$ and $SubG_3$ should be swapped because $m_{13} > m_{12}$ when fixing the order of the $SubG_1$. We can observe that our greedy Reorder strategy further reduces the memory traffic between CPU and GPU.

4.2 Memory-Aware Computation

As discussed in Section 3.2, the low L1/L2 cache hit rate incurred by irregular memory accesses during the aggregation limits the GPU performance and slows down the computation phase. As presented in Equation 1, the features of the source node (x_v), weight w_{uv} and partial sums (\hat{h}_u) of the hidden features h_u participate in the aggregation of the target node u . In the naive case (e.g., DGL and PyG), all the above data is stored in the low-bandwidth global memory and is first fetched to high-bandwidth L1 cache when it is requested. However, as shown in Figure 7a, due to the extreme sparsity and the massive data size, the fetched data may no longer be used and will be evicted to free up memory for other requested data, which results in the underutilization of the L1 cache and then impedes the overall bandwidth and GPU performance. Intuitively, storing all required data in the L1 cache would maximize the performance. However, two challenges exist: (1) We cannot store the data in the L1 cache explicitly because the L1 cache is not software-managed. (2) The capacity of the L1 cache is too small (e.g., 128KB per SM in 3090 GPU) to accommodate all required data.

Accordingly, we propose the **Memory-Aware** computation method by employing the customizable shared memory provided by GPU, which has the same bandwidth and capacity as the L1 cache. The key idea is that we adjust the memory access pattern in the aggregation phase and prioritize the storage of frequently accessed data in higher-bandwidth memory to maximally increase the overall bandwidth available to the computing units, thus boosting the GPU performance.

We first analyze the access frequencies of different data. To complete the aggregation of node u , the features of each source node (x_v) are read one time, w_{uv} for the node v is read d times where d is the dimension of the nodes features, and \hat{h}_u is read $|N(u)| - 1$ times to perform the accumulation. The access frequencies of \hat{h}_u and w_{uv} significantly exceed that of x_v because the number of neighbors ($|N(u)|$) is often 5, 10

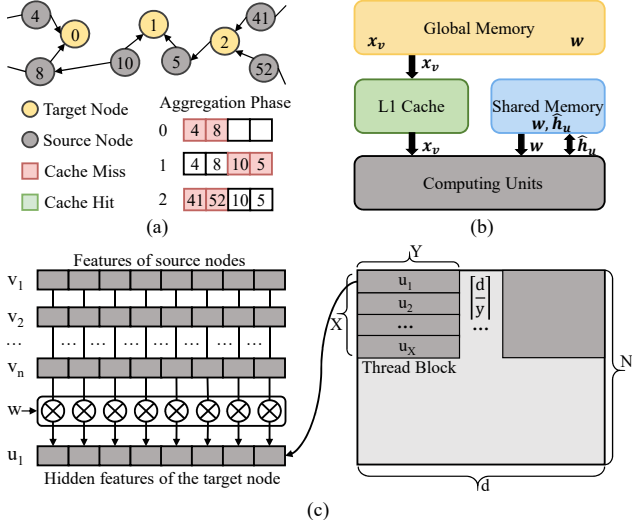


Figure 7. (a) An example of the L1 cache utilization during the aggregation in the naive case. (b) The memory access pattern of our proposed Memory-Aware computation method. (c) The aggregation utilizing threads parallelism on GPU (N is the total number of target nodes). \otimes denotes the Fused Multiply Add operation.

or 15 and d is always large (e.g., 256 or 512). Based on this analysis, the partial sums \hat{h}_u and the weight w_{uv} are stored in the shared memory with higher bandwidth, and x_v with a lower access frequency is stored in the lower-bandwidth global memory, as shown in Figure 7b. Then computing units fetch the data from its corresponding memory. With the same lifespan as the thread block, the shared memory only stores the data required by the corresponding thread block, decreasing the memory capacity burden. Moreover, to guarantee the correctness of the aggregation, the aggregation of a specific target node u must be completed in one thread block.

To further illustrate the efficiency of our Memory-Aware method, we quantitatively analyze the memory access time as follows. We assume that the bandwidth of the shared memory (L1 cache) and the global memory are B_s and B_g , respectively, and the data is all in FP32 format. We omit the time of accessing the L1/L2 cache for simplicity. In the naive case, all data should be read from the low-bandwidth global memory and the time of fetching data when aggregating the node u is:

$$t_n = \frac{4(|N(u)| - 1)d + 4|N(u)|d + 4|N(u)|d}{B_g}. \quad (3)$$

With the Memory-Aware method, we can fetch the most accessed data, i.e., partial sums and weights, from the higher-bandwidth shared memory and the access time is:

$$t_m = \frac{4(|N(u)| - 1)d + 4|N(u)|(d - 1)}{B_s} + \frac{4|N(u)|d + 4|N(u)|}{B_g}. \quad (4)$$

Given that $B_s \gg B_g$, t_m is notably less than t_n ($\sim 10\times$). The Memory-Aware method effectively diminishes memory access time and curtails the idle periods of computing units

caused by delays in data retrieval, substantially improving the GPU performance and accelerating the computation.

Similar to the forward pass of the aggregation, the target node also gathers information from its neighbors to complete the backward pass, where the information is the gradient of the loss function with respect to node feature:

$$\frac{\partial L}{\partial \mathbf{h}_u} = \sum_{v \in N(u)} w_{uv} \cdot \frac{\partial L}{\partial \mathbf{x}_v}. \quad (5)$$

Therefore, we also apply the Memory-Aware method to the backward phase to further accelerate the computation phase.

Thread block settings: To efficiently support the fine-grained control of memory accesses, we develop the customized CUDA kernel to perform the aggregation phase instead of adopting the traditional GeMM kernel. As shown in Figure 7c, we first set each thread block of the kernel to be responsible for the concurrent aggregation of X target nodes. To improve the parallelism of the computation, each thread is responsible for the aggregation of one dimension of the hidden features. Because the upper limit of the threads allowed by a thread block is 1024 in current GPU hardware, we constrain the Y -dimensional features processed by each thread block to suffice $X \cdot Y < 1024$, and use $\lceil \frac{d}{Y} \rceil$ thread blocks to complete the aggregation of all hidden features of these X target nodes.

When the kernel performs the aggregation, it first fetches the corresponding features of source nodes from the global memory and the weights from the shared memory. Then the kernel conducts the multiplication to obtain the weighted features. Finally, it fetches the corresponding partial sums (\hat{h}_u) from the shared memory and adds the weighted features with \hat{h}_u together to get the updated \hat{h}_u and then writes it to the shared memory. Note that there is no requirement for thread synchronizations because each thread is only responsible for one dimension of the hidden features and performs the accumulation independently. Each thread block only needs to store the $X \cdot Y$ -dimensional partial sums and the weights required by the X target nodes in the shared memory. The target node u needs $|N(u)|$ weights. Therefore, the capacity requirement of the shared memory for each thread block is $4XY + 4X|N(u)|$, where $4XY$ and $4X|N(u)|$ are used to stored the partial sums and weights, respectively. Through setting the appropriate values of X and Y , we ensure the size of the shared memory required by each thread block to satisfy the hardware limitation and keep the maximum occupancy of the SM. We empirically set $X = 8$ and $Y = 32$.

4.3 Fused-Map Sampling

As our analysis in Section 3.3, due to the extensive thread synchronizations to obtain local IDs in the ID map process, the sample phase emerges as the principal performance bottleneck after optimizing the memory IO and computation. To alleviate this problem, we propose the **Fused-Map** sampling

Algorithm 2 Fused-Map Algorithm

```

1: Initialize: HashTable: record the mapping (global ID  $\rightarrow$  local ID) and enable fast indexing the mapping by global ID, we initialize the keys of the HashTable to -1 and the values to 0; LocalID = 0: record the current local ID.
2: atomicCAS(address, OldValue, NewValue):
3:   ReturnVal = HashTable[HashIndex].key
4:   if HashTable[HashIndex].key == OldValue
5:     HashTable[HashIndex].key == NewValue
6:   end if
7:   return ReturnVal
8: end
9: InsertID(GlobalID):
10:  InsertSucceed = False
11:  HashIndex = HashFunction(GlobalID)
12:  while InsertSucceed == False:
13:    Val = atomicCAS(HashIndex, -1, GlobalID)
14:    if Val == GlobalID || Val == -1 then
15:      InsertSucceed = True
16:      Flag = (Val == -1) ? True : False
17:    else
18:      # There is a conflict at the location of HashIndex
19:      # The other GlobalID has been inserted at HashIndex
20:      HashIndex = HashIndex + 1
21:      # Do the linear probing until the insertion successes
22:    end if
23:  return HashIndex, Flag
24: end
25: Fused Map(GlobalID):
26:  HashIndex, Flag = InsertID(GlobalID)
27:  if Flag == False then
28:    HashTable[HashIndex].value = LocalID
29:    atomicAdd(LocalID, 1)
30:  end if
31: end

```

method, which avoids the costly thread synchronizations by fusing the calculation of local IDs with the construction of the hash table in the ID map process.

Algorithm 2 presents our Fused-Map method. The *key* of the item in the *HashTable* stores the global ID and the *value* stores the local ID (line 1). *LocalID* records the number of unduplicated global IDs that have been processed, i.e., the current local ID. To construct the hash table, the *InsertID* function (line 26) inserts the global ID into the *HashTable* as the *key* of one item, whose location is calculated by a *Hash-Function*, such as the mod computation (line 11). Note that the insertion is atomic to ensure that the same location of the hash table can only be accessed by a single thread at a time, which is implemented by the *atomicCAS* function provided by CUDA, as shown in line 13. The details of the *atomicCAS* are shown in lines 2-8, where the operations are performed in one atomic transaction. Moreover, to resolve the potential hash conflicts, we utilize the linear probing to find the inserted location until the insertion succeeds (line 20). If there is no conflict and the global ID has not been inserted, we

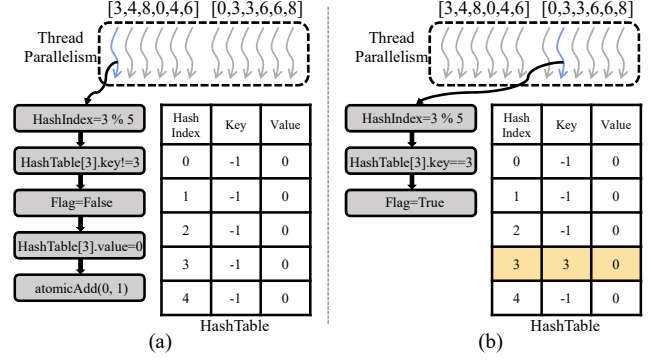


Figure 8. An example of the Fused-Map process.

insert the global ID into the *HashTable* (line 5) and assign the corresponding boolean value to the *Flag* (line 16) according to the returned value of the *atomicCAS*. The *Flag* indicates whether the item at *HashIndex* has been assigned the same global ID or has not been inserted. The *Flag* is set to *False* if there is no identical global ID at *HashIndex*, otherwise the opposite. If *Flag* is *False*, it means that the current inserted global ID represents a new node, we assign the value of *LocalID* to the *value* of the item at *HashIndex* (line 28), i.e., construct a mapping between the global ID (*key*) and the local ID (*value*). Then, the *LocalID* is incremented by 1 (line 29). If *Flag* is *True*, it means that other threads have processed this global ID, and we do not perform any operation. Considering that the above process is executed in a large number of threads concurrently, in order to guarantee the *LocalID* to be accumulated correctly, we adopt the *atomicADD* to perform the accumulation.

With the Fused-Map approach, we construct the hash table while obtaining the mappings between the local IDs and the global IDs without any thread synchronization in the same CUDA kernel, thus significantly accelerating the sample process. After the construction is done, we launch another kernel and transform global IDs to local IDs by fast indexing the mapping with global ID and then complete the ID map.

Figure 8 illustrates an example of the Fused-Map process. We use $\text{HashIndex} = \text{id} \% 5$ (5 is the size of the *HashTable*) as the *HashFunction* and employ the linear probing to resolve collisions in the hash table. The initial value of *LocalID* is 0. In Figure 8a, the thread atomically inserts the global ID 3 into the *HashTable* and the global ID 3 has not been processed, thus the *Flag* is *False*. And then we assign the current *LocalID* to the *value* of the corresponding item in the *HashTable* and obtain the mapping between global id 3 and its local id 0. As shown in Figure 8b, when other threads try to insert global ID 3 into the table, this global ID has been processed, thus *Flag* is *True* and we do not perform any operation.

Discussion: The users may be concerned about the maximum graph size (i.e., the number of nodes) that our Fused-Map can support due to the usage of the atomic functions (*atomicADD* and *atomicCAS*). For the insertion of the pair of key and value, only the insertion of the key is atomic and the insertion of the value is determined by the returned

Table 5. The configurations of the compared frameworks.

Frameworks	Sample Device	Sample Optimization	Memory IO Optimization	Computation Optimization
PyG	CPU	No	Prefetch	No
DGL	GPU	No	Prefetch	No
GNNAdvisor	No	No	No	2D workload management
GNNLab	GPU	Parallel	Cache	No
FastGL	GPU	Fused-Map	Match-Reorder	Memory-Aware

value of the *atomicCAS* (line 27-28). And the accumulation of the *LocalID* is performed in a different atomic transaction, i.e., *atomicADD*. According to the programming guide from NVIDIA [6], the *atomicADD* and *atomicCAS* both support 64-bit variants. Accordingly, our Fused-Map method can support the sampling of graphs with up to 2^{64} nodes, which would be sufficient for the GNNs and graph community in the foreseeable future.

5 Implementation

We implement our FastGL using the PyTorch [29] as the back-end deep learning framework. We reuse the data loader of the open-sourced Deep Graph Library (DGL v1.0.0 [38]) to load the graph datasets and the sampled subgraphs. To perform our Match-Reorder strategy, we implement two Python classes, *reorder()* and *match()*, to perform the Greedy Reorder Strategy and the Match process, respectively. When there is sufficient GPU memory left, FastGL also utilizes a portion of GPU memory as a cache to further accelerate the memory IO as GNNLab [43]. We customize CUDA kernel functions to achieve fine-grained control over memory access in the Memory-Aware computation and warp these functions into user-friendly APIs, i.e., *A3.forward()* and *A3.backward()*, which are conveniently adopted to build layers for various GNN models. We reconstruct the sampler through the proposed Fused-Map sampling method in CUDA and integrate this sampler with the data loader of DGL. We adopt the NCCL [7] to perform the gradient synchronization and implement the data parallel sampling-based GNN training on multiple GPUs in one machine. With the warped user-friendly APIs, each contribution in our design can also be conveniently applied to improve other frameworks with minimal change.

6 Evaluation

6.1 Experiment Setup

Benchmarks: We choose three representative GNN models widely used to evaluate the framework as previous works [25, 26, 43]: Graph Convolutional Network (GCN) [21], Graph Isomorphism Network (GIN) [41] and Graph Attention Network (GAT) [33]. These models all adopt 3-hop random neighborhood sampling [50] and the number of sampled neighbors for different layers are 5, 10, and 15, respectively, following the settings in GNNLab [43]. In addition, we set the batch

Table 6. The statistics of datasets used in this work (M: Million, B: Billion).

Dataset	Nodes	Edges	Features	Classes
Reddit	232,965	0.11B	602	41
Products	2.44M	123M	200	47
MAG	10.1M	0.3B	100	8
IGB-large	100M	1.2B	1024	19
Papers100M	111M	1.61B	128	172

size to 8000 as GNNLab [43]. The feature dimension of the hidden layers of GCN and GIN is 64, and the hidden layer of GAT has eight heads and the dimension of each head is 8.

Datasets: We evaluate our FastGL on five real-world graph datasets with various scales as shown in Table 6. The Reddit (RD) is from [12]. The Products (PR) and Papers100M (PA) are provided by Open Graph Benchmark (OGB) [13]. The Products is a co-purchasing network, and the Papers100M is a citation network. Obtained from the Illinois Graph Benchmark (IGB) [20], IGB-large (IGB) graph is a collection of academic graphs. The MAG processed by [1] is a graph that contains scientific publication records and citation relationships between those publications.

Baselines*: We compare FastGL with the state-of-the-art PyG 2.1.0 [23], DGL 1.0.0 [38], GNNAdvisor [39] and GNNLab [43]. Table 5 presents the configurations of these compared frameworks. PyG conducts sampling on the CPU. However, DGL utilizes GPU to accelerate the sample phase. PyG and DGL both optimize the memory IO by prefetching. GNNLab proposes a more efficient cache policy to reduce data traffic and performs the sample and computation in parallel on different GPUs to accelerate the training. GNNLab significantly outperforms other GNN frameworks [23, 25, 38]. We make an in-depth comparison with GNNLab in our evaluation. Dedicated to the full-graph training, GNNAdvisor can not support sampling. To compare against the GNNAdvisor, we integrate the sampler of DGL into the GNNAdvisor to enable it to support the sampling-based GNN training. GNNAdvisor first preprocesses the graph according to the properties of the GNN and graph. Then it accelerates the computation by its 2D workload management. In the full-graph training scenario, the preprocess is just performed once before training, and the preprocessing time can be significantly amortized by the multiple training epochs (e.g., 200). Therefore, the preprocessing time can be overlooked. However, for the sampling-based training, only after the sampled subgraphs are preprocessed, can the computation be performed in each iteration, i.e., each iteration needs preprocessing. Thus the preprocessing time must be included in the overall end-to-end training time to ensure a fair comparison with other sampling-based training systems. All results are the average values over 20 epochs.

*We use all baselines' open-sourced implementations.

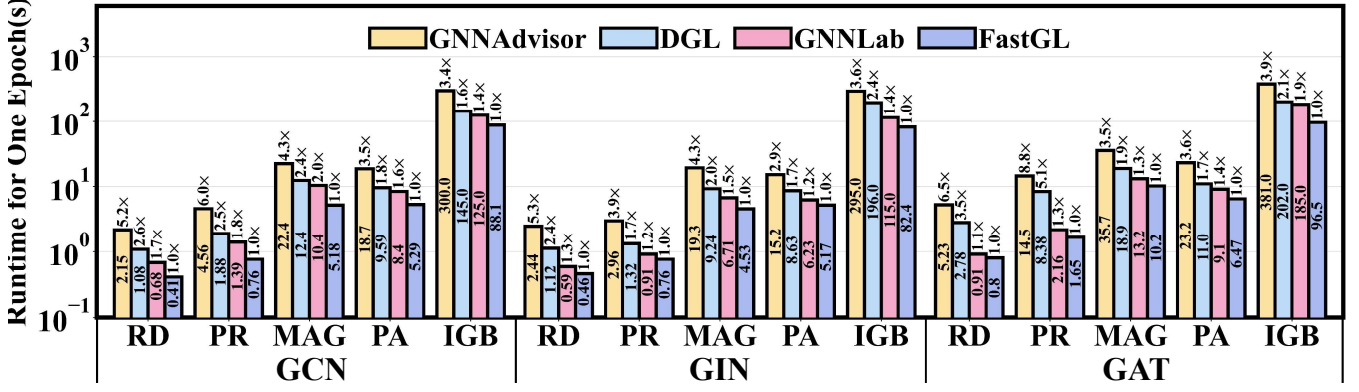


Figure 9. The training speed of three GNN models at various datasets on 2 GPUs compared with baselines. The numbers above bars are speedups of FastGL over baselines. The numbers in bars are the absolute times of one epoch.

Environment: All evaluations are performed on a GPU server that consists of two AMD EPYC 7532 CPUs (total 2×32 cores), 512GB DRAM, and eight NVIDIA GeForce RTX 3090 (with 24GB memory) GPUs. The software environment of the server is configured with Python v3.7.13, PyTorch v1.10.1, CUDA v11.0, DGL v1.0.0, and PyG v2.1.0.

6.2 Overall Performance

As shown in Figure 9, we compare the training speed with baselines on three GNN models over various datasets. The time is measured on 2 GPUs because GNNLab has to run on at least 2 GPUs to obtain optimal performance where one GPU is to sample and the other one to perform the computation.

By accelerating the memory IO, sample, and computation phases simultaneously, FastGL significantly outperforms PyG, DGL, GNNAdvisor and GNNLab by up to $28.9\times$ (from $4.3\times$), $5.1\times$ (from $1.7\times$), $8.8\times$ (from $2.9\times$) and $2.0\times$ (from $1.1\times$), respectively. We do not plot the results of PyG in Figure 9 because PyG is more than an order of magnitude slower than our FastGL. The speedup over PyG is especially significant because PyG performs the sampling on the CPU, which is ill-suited to large-scale graph scenarios that require massive parallel operations, resulting in the sample phase occupying up to 97% of the overall time. Our FastGL optimizes the sampling by the Fused-Map method, which fully takes advantage of the thread parallelism on GPU and considerably reduces the sampling time. DGL also accelerates the sample utilizing GPU, but the vast volume of thread synchronizations still hinder the acceleration of sampling, which is tackled well by our FastGL. Compared with GNNLab, FastGL also obtains substantial speedups. Although GNNLab optimizes the memory IO phase, the benefits discount on large-scale graphs where there is no extra GPU memory to be used as a cache (e.g., MAG and PA). However, on these datasets, FastGL also achieves considerable speedups thanks to the Match-Reorder strategy, which significantly reduces the data traffic without any extra GPU memory. Although GNNAdvisor optimizes

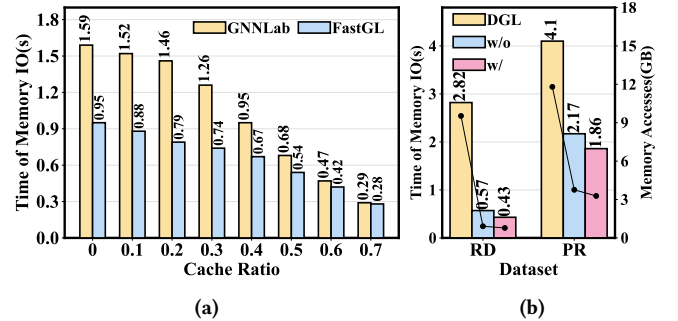


Figure 10. The time spent on the memory IO comparison between (a) GNNLab and FastGL of GCN on Products; (b) with and without the Greedy Reorder Strategy on GCN (measured on one GPU).

the computation phase, the necessary preprocess in each iteration incurs significant time overhead, which leads to GNNAdvisor performing poorly in the sampling-based training scenario. However, by utilizing our Memory-Aware method without any preprocessing, FastGL accelerates the computation and further boosts the overall training process. Additionally, FastGL consistently obtains significant speedups on all three GNN models, which demonstrates the generalization of our FastGL.

6.3 Performance Breakdown

To analyze where our gains come from and demonstrate the effectiveness of our three proposed techniques separately, we conduct more detailed breakdown analyses.

1) The effectiveness of the Match-Reorder strategy: The Match-Reorder is proposed to reduce the data traffic without imposing any GPU memory cost. We compare the time of memory IO with GNNLab under different memory capacity remaining situations, as shown in Figure 10a. We cache a portion of nodes features into GPU memory (referred to as *cache ratio*) to simulate how much GPU memory is left. For example, *cache ratio* = 0 represents that there is no GPU

Table 7. The comparison of time spent on memory IO between DGL and FastGL on GCN on 1 GPU when employing the random walk sampler. ‘FastGL-nG’ denotes the situation without our Greedy Reorder Strategy. Values in () are normalized speedup ratios.

	RD	PR	MAG	PA
DGL	1.91s (1.0)	1.92s (1.0)	16.4s (1.0)	4.18s (1.0)
FastGL-nG	0.75s (2.6)	1.30s (1.5)	15.1s (1.1)	3.89s (1.1)
FastGL	0.65s (2.9)	1.16s (1.7)	13.1s (1.3)	3.54s (1.2)

memory to be used as the cache, and $cache\ ratio = 0.1$ represents that there is $0.1 \cdot M$ memory left on GPU, where M is the total size of the nodes features. In large-graph scenarios, there is often a little memory left to be used as the cache ($cache\ ratio < 0.5$) and Figure 10a reveals that our Match-Reorder approach significantly reduces the time of the memory IO in these situations, which demonstrates the superiority of our Match-Reorder strategy. Additionally, when sufficient GPU memory is available for caching, our method also has a minor improvement over GNNLab. We also explore the impact of the Greedy Reorder Strategy on the memory IO time. As shown in Figure 10b, without the Greedy Reorder Strategy, FastGL still obtains significant speedups compared to DGL (‘w/o’ v.s. ‘DGL’) thanks to our proposed Match process. The solid lines represent the average number of memory accesses per epoch. Moreover, equipped with the Greedy Reorder Strategy (‘w/’), FastGL accelerates the memory IO phase by up to 25% compared with the situation only with the Match process (‘w/o’) because our Greedy Reorder Strategy maximizes the reuse of the overlapping nodes between different mini-batches and further reduces the data traffic based on the Match process.

The efficiency of our Match-Reorder strategy is highly related to the match degrees between different subgraphs, which are determined by the sampling algorithm. To illustrate the broad applicability of our approach, we compare the time spent on memory IO phase of FastGL and DGL on GCN when employing the random walk algorithm to sample. We set the hyperparameters of the random walk sampler (length is 3) as the PinSAGE [46] used, which is a GNN for web-scale recommender systems. As shown in Table 7, our FastGL can still accelerate the memory IO phase, which demonstrates the broad applicability of our Match-Reorder method. Moreover, the comparison between ‘FastGL-nG’ and ‘FastGL’ shows that our Greedy Reorder Strategy can also be applied to other sampling algorithms.

2) The superiority of the Memory-Aware computation: As shown in Figure 11, we compare the computation time with DGL, PyG, and GNNAdvisor. We can observe that our Memory-Aware method significantly outperforms the three frameworks on all graph datasets with $1.1\times$ to $6.7\times$

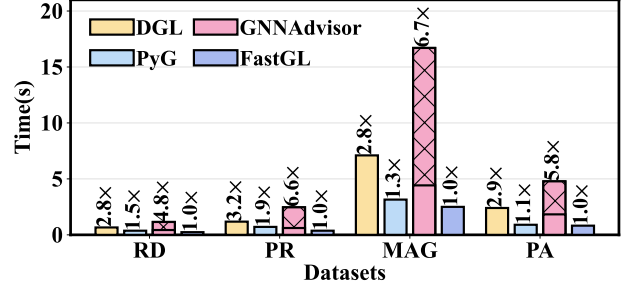


Figure 11. The time spent on the computation phase comparison on GCN with 2 GPUs.

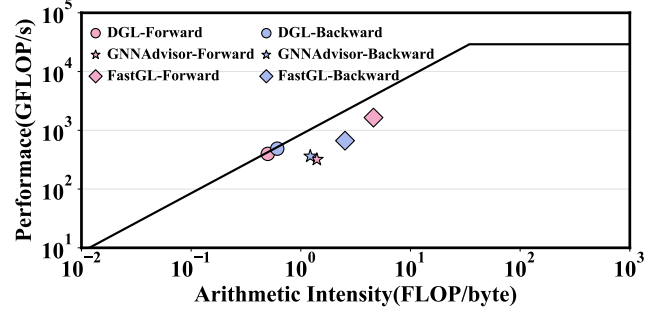


Figure 12. Roofline analyses of the computation phase of GCN in different frameworks on Products dataset.

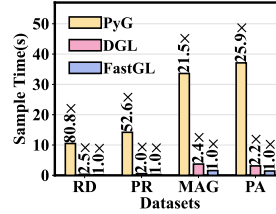


Figure 13. Sample time of each epoch comparison on GCN.

Table 8. The spent time (s) comparison between DGL and our Fused-Map method during the ID map process.

	DGL	Fused-Map
RD	0.18(2.3×)	0.08(1×)
PR	0.30(2.1×)	0.14(1×)
MAG	2.55(2.6×)	0.98(1×)
PA	2.18(2.7×)	0.81(1×)

speedup in the computation phase. GNNAdvisor has a negative effect on accelerating the computation phase because it is dedicated to the full-batch training and requires pre-processing the graph. In the full-batch training scenario, the preprocess only performs once and the overhead can be amortized by multiple training epochs (e.g., 200). However, for the large-scale graph where sampling-based training is necessary, the preprocess is performed for each sampled subgraph, and thus the overhead of preprocessing cannot be amortized. The shadowed top part of the GNNAdvisor bar in Figure 11 displays the preprocessing time, which occupies up to 75% of the overall computation process and results in the significant deceleration of the computation phase. Furthermore, to demonstrate the effectiveness of improving the GPU performance, we also perform the roofline analyses for the forward and backward pass of the aggregation phase, as shown in Figure 12. Our FastGL achieves up to $4.2\times$ higher actual performance compared with DGL and GNNAdvisor.

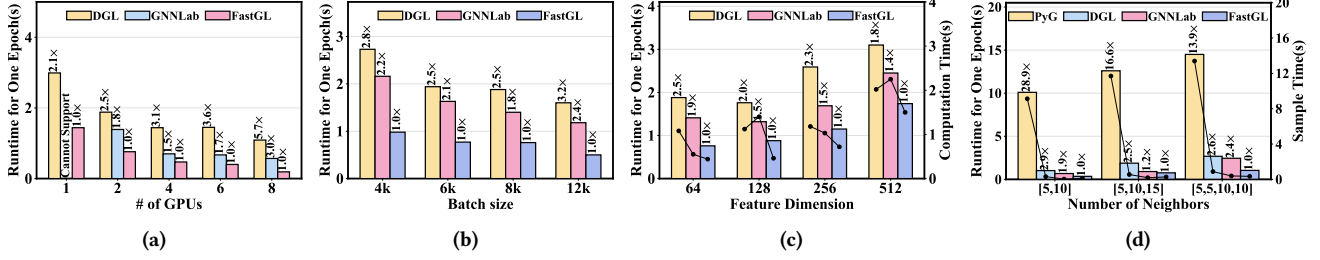


Figure 14. (a) Scalability on the number of GPUs. (b) Scalability on the batch size. (c) Scalability on the feature dimension. (d) Scalability on the number of sampled neighbors and the layers ($[N_1, N_2, \dots, N_k]$ represents there are k layers and the sampled neighbors for the k -th is N_k).

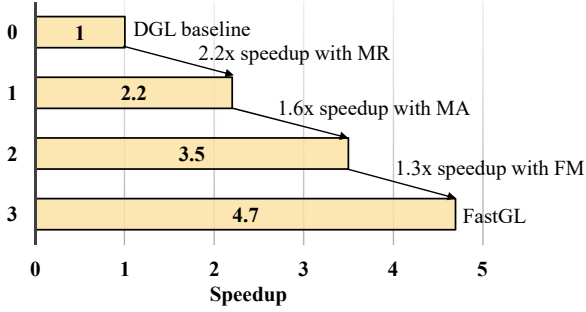


Figure 15. The breakdown analysis on the average overall speedup across all five datasets on GCN using 2 GPUs. ‘MR’ denotes Match-Reorder, ‘MA’ denotes Memory-Aware, and ‘FM’ denotes Fused-Map.

Note that our Memory-Aware method do not change the total accessed size of data from GPU memory to computing units during the computation phase. However, through improving the achievable bandwidth by storing the more frequently accessed data in the memory with a higher bandwidth, the memory access time of the computation phase is significantly reduced, which accelerates the computation.

3) The benefits from the Fused-Map sample: The sample phase time comparison with DGL and PyG on GCN (running on 2 GPUs) is shown in Figure 13. The sampling speed in FastGL is much faster than PyG (up to 80.8× speedup). Compared with DGL, our FastGL can also obtain up to 2.5× (from 2.0×) speedup because the Fused-Map sample avoids the vast volume of thread synchronizations to calculate the local IDs, which is the main bottleneck in the sampling by GPU. Moreover, Table 8 indicates that our Fused-Map sample method significantly reduce the time spent on the ID map process by the fused mechanism.

4) The ablation study on where the performance gains from: We conduct a breakdown analysis on the overall speedup to analyze how our three proposed techniques separately affect the overall speedup. As shown in Figure 15, we run this experiment on GCN using the five datasets and adopting DGL as the baseline. We can observe that optimizing the memory IO phase by our Match-Reorder method significantly reduces the overall training time because the memory IO phase dominates the training process, as we analyze in

Section 3.1. Our Memory-Aware computation manner also brings 1.6× speedup gain by efficiently improving the achievable bandwidth of the computing units. The gains from the Fuse-Map method are relatively low compared to the above two, because the time spent on sampling is a small fraction (31%-51%) of the overall training time.

6.4 Scalability

To demonstrate the generalization of our FastGL, we conduct the scalability experiments using different settings on GPU and GNN models. If not specified, the GNNs used to evaluate are all set as described in Section 6.1, with a batch size of 8000 trained on Products with 2 GPUs.

1) The scalability on the number of GPUs: Figure 14a displays the experimental results using different numbers (n) of GPUs. When running on 1 GPU, we only evaluate on DGL and FastGL because GNNLab cannot support the training on 1 GPU. For GNNLab, we utilize 1 GPU to sample when $n \leq 4$ (the others to compute) and 2 GPUs to sample when $n > 4$ to obtain the optimal performance of GNNLab. In general, FastGL consistently outperforms other frameworks when the GPU number increases. Moreover, as the number of GPUs increases, the speedups over baselines are more significant, which shows better scalability of FastGL. Across all datasets, when using 8 GPUs, DGL and FastGL on-average obtain 3.36× and 5.93× speedups over that on 1 GPU, respectively.

2) The scalability on the batch size: We also explore how the batch size affects the training speed. As shown in Figure 14b, FastGL obtains 1.8× to 3.2× speedup with different batch sizes compared to baselines. We can observe that FastGL achieves higher speedup with larger batch sizes (e.g., 12k v.s. 6k). The reasons are twofold: (1) When batch size is larger, there are more overlapping nodes between different mini-batches and our Match-Reorder strategy can reduce more data traffic. (2) As the batch size increases, the sample phase becomes the main bottleneck, which is significantly accelerated by our Fused-Map sample method.

3) The scalability on the feature dimension: Figure 14c presents the effect of feature dimension on the training speed (bar) and the computation speed (solid line) using different

Table 9. The comparison of the GPU memory usage on GCN over various datasets on 1 GPU.

	RD	PR	MAG	IGB	PA
DGL	6257MB	9853MB	20085MB	23447MB	14030MB
FastGL	5217MB	7705MB	19893MB	21035MB	14629MB

frameworks. The training speed of FastGL consistently outperforms the other frameworks ($1.4\times$ to $2.5\times$) when adopting different feature dimensions. The experimental results on computation speed demonstrate that our Memory-Aware method is effective for various feature dimensions.

4) The scalability on the number of sampled neighbors and the hops: We also investigate the impact of sampled neighbors and the layers on the overall time (bar) and the sample time (solid line) in Figure 14d. With different numbers of layers and sampled neighbors, FastGL obtains $1.2\times$ to $28.0\times$ training speedups over baselines, which demonstrates the robustness of FastGL. Moreover, the speed of sampling using FastGL is significantly higher than PyG and DGL, thanks to the fused ID map process. The sampling speed of FastGL is comparable to that of GNNLab on ‘[5,10]’ and ‘[5,10,15]’ because GNNLab runs the sample and computation in parallel on different GPUs where the latency of sampling is hidden by the computation. However, when the size of the sampled subgraph increases (‘[5,5,10,10]’), the latency cannot be hidden by the computation well, where our FastGL spends significantly less time sampling than GNNLab.

6.5 Memory Trade-Off Analysis

To analyze the memory overhead of our FastGL, we compare the GPU memory usage of the GCN model at various datasets on 1 GPU with DGL. As shown in Table 9, the memory usage of the two systems is comparable, which demonstrates that the memory overhead induced by our methods is not significant. The reasons are twofold: (1) The metadata used in our Fused-Map is also used in the DGL system, e.g., the hash table. (2) In our Reorder strategy, we only store the topology information of the currently processed subgraph on the GPU and the others in the host memory, which would not increase the GPU memory usage compared with DGL. Note that we prefetch the topology information of the next subgraph, whose time can be perfectly overlapped by the computation because its size (without nodes features) is minimal.

6.6 Training Convergence

To confirm the correctness of our FastGL, we evaluate the training loss of training two GNN models (i.e., GCN and GIN) with FastGL and DGL (baseline) over Reddit on 2 GPUs. As shown in Figure 16, FastGL converges to approximately the same loss as the original DGL when completing the overall training process (training one mini-batch is an iteration).

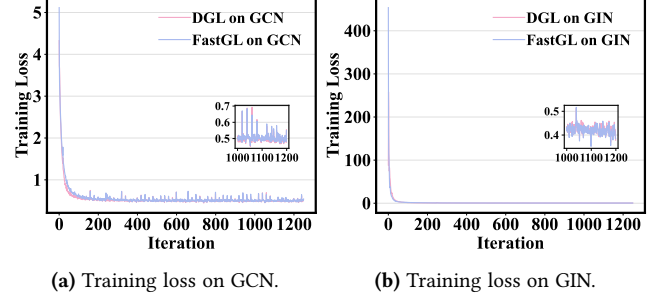


Figure 16. The training loss of FastGL and DGL on Reddit dataset of GCN and GIN models.

7 Discussion

1)The broader applicability of our FastGL: In this work, we focus on the acceleration of sampling-based GNN training on a single machine with multiple GPUs. Nonetheless, we expect that FastGL is also efficient on multiple machines because the mechanism of our three contributions proposed in this paper are irrelevant of the number of machines. Moreover, besides the random neighborhood sampling algorithm mainly used in our evaluation, our Fused-Map method can also be employed to accelerate diverse sampling algorithms since they all need to transform the global ID to the local ID (ID map process) to update the subgraph structures [3, 4, 12, 15, 30, 48, 51].

2)The difference between our Match-Reorder and NextDoor[16]: NextDoor and our Match-Reorder method both are based on the observation that the same node may appear in different sampled subgraphs. However, we develop completely different methods. NextDoor assigns the overlapping node to the same grid block to realize coalesced global memory accesses and accelerate the sampling phase. Differently, we first develop the Match strategy to reuse the overlapping nodes between subgraphs to reduce the data traffic between CPU and GPU and accelerate the memory IO phase. Then, the greedy Reorder strategy is proposed to maximize this reduction.

3)The future direction of accelerating the sampling-based GNN training: Our work reveals that the memory IO phase dominates the overall sampling-based GNN training process now. The memory IO phase consists of two stages: (1) organize the data on the CPU side to ensure they are consecutive in the memory; (2) transfer the data from CPU to GPU. A fact that cannot be ignored is the increasing bandwidth between the GPU and the host, e.g., the upcoming widely used next-generation architecture, NVidia’s Grace Hopper, holds up to 900GB/s of bandwidth [8]. In this situation, the time spent on stage (2) may not be significant, and the bottleneck would shift toward stage (1). Therefore, optimizing the way data is organized on the CPU side may be able to lead to new performance breakthroughs in the future.

8 Conclusion

In this paper, we propose FastGL, a GPU-efficient GNN training framework for large-scale graphs that simultaneously accelerates the memory IO, computation, and sample phases. Specifically, we propose the Match-Reorder strategy to accelerate the memory IO by reusing the overlapping nodes between different mini-batches without requiring any extra GPU memory, which is well suited to the training on large-scale graphs. Moreover, we put forward the Memory-Aware computation method, which redesigns the memory access pattern during the computation to increase the overall bandwidth utilization, thus improving the GPU performance and accelerating the computation phase. Finally, we also present a Fused-Map sampling approach to avoid the thread synchronizations and accelerate the sample phase through a fused mechanism. Extensive experiments compared with the prior art demonstrate the superiority of our FastGL.

9 Acknowledgments

We extend our gratitude to the the ASPLOS reviewers who participated in the evaluation of FastGL for their valuable insights and feedback. This work was supported in part by the STI 2030-Major Projects (No.2021ZD0201504), the Jiangsu Key Research and Development Plan (No.BE2021012-2), the National Natural Science Foundation of China (No.62106267), the Key Research and Development Program of Jiangsu Province (Grants No.BE2023016) and the Beijing Municipal Science and Technology Project (No.Z231100010323002).

References

- [1] Aleksandar Bojchevski, Johannes Gasteiger, Bryan Perozzi, Amol Kapoor, Martin Blais, Benedek Rózsemberczki, Michal Lukasik, and Stephan Günnemann. Scaling graph neural networks with approximate pagerank. In *Proceedings of the 26th ACM SIGKDD International Conference on Knowledge Discovery & Data Mining*, pages 2464–2473, 2020. doi:<https://doi.org/10.1145/3394486.3403296>.
- [2] Zhenkun Cai, Qihui Zhou, Xiao Yan, Da Zheng, Xiang Song, Chengguang Zheng, James Cheng, and George Karypis. Dsp: Efficient gnn training with multiple gpus. In *Proceedings of the 28th ACM SIGPLAN Annual Symposium on Principles and Practice of Parallel Programming*, pages 392–404, 2023. doi:<https://doi.org/10.1145/3572848.3577528>.
- [3] Jianfei Chen, Jun Zhu, and Le Song. Stochastic training of graph convolutional networks with variance reduction. In *International Conference on Machine Learning*, pages 942–950. PMLR, 2018. doi:<https://doi.org/10.48550/arXiv.1710.10568>.
- [4] Jie Chen, Tengfei Ma, and Cao Xiao. Fastgcn: Fast learning with graph convolutional networks via importance sampling. In *International Conference on Learning Representations*, 2018. doi:<https://doi.org/10.48550/arXiv.1801.10247>.
- [5] Wei-Lin Chiang, Xuanqing Liu, Si Si, Yang Li, Samy Bengio, and Chong-Jui Hsieh. Cluster-gcn: An efficient algorithm for training deep and large graph convolutional networks. In *Proceedings of the 25th ACM SIGKDD international conference on knowledge discovery & data mining*, pages 257–266, 2019. doi:<https://doi.org/10.1145/3292500.3330925>.
- [6] NVIDIA Corporation. Cuda c++ programming guide, <https://docs.nvidia.com/cuda/cuda-c-programming-guide/index.html>, 2023.
- [7] NVIDIA Corporation. Nvidia collective communications library (nccl), 2023.
- [8] NVIDIA Corporation. Nvidia grace hopper superchip architecture whitepaper, <https://resources.nvidia.com/en-us-grace-cpu/nvidia-grace-hopper>, 2023.
- [9] Wenqi Fan, Yao Ma, Qing Li, Yuan He, Eric Zhao, Jiliang Tang, and Dawei Yin. Graph neural networks for social recommendation. In *The world wide web conference*, pages 417–426, 2019. doi:<https://doi.org/10.1145/3308558.3313488>.
- [10] Matthias Fey and Jan Eric Lenssen. Fast graph representation learning with pytorch geometric. *arXiv preprint arXiv:1903.02428*, 2019. doi:<https://doi.org/10.48550/arXiv.1903.02428>.
- [11] Swapnil Gandhi and Anand Padmanabha Iyer. P3: Distributed deep graph learning at scale. In *15th {USENIX} Symposium on Operating Systems Design and Implementation ({OSDI} 21)*, pages 551–568, 2021.
- [12] Will Hamilton, Zhitaoying Ying, and Jure Leskovec. Inductive representation learning on large graphs. *Advances in neural information processing systems*, 30, 2017. doi:<https://dl.acm.org/doi/10.5555/3294771.3294869>.
- [13] Weihua Hu, Matthias Fey, Marinka Zitnik, Yuxiao Dong, Hongyu Ren, Bowen Liu, Michele Catasta, and Jure Leskovec. Open graph benchmark: Datasets for machine learning on graphs. *Advances in neural information processing systems*, 33:22118–22133, 2020. doi:<https://dl.acm.org/doi/10.5555/3495724.3497579>.
- [14] Chengying Huan, Shuaiwen Leon Song, Yongchao Liu, Heng Zhang, Hang Liu, Charles He, Kang Chen, Jinlei Jiang, and Yongwei Wu. T-gcn: A sampling based streaming graph neural network system with hybrid architecture. In *Proceedings of the International Conference on Parallel Architectures and Compilation Techniques*, pages 69–82, 2022. doi:<https://doi.org/10.1145/3559009.3569648>.
- [15] Wenbing Huang, Tong Zhang, Yu Rong, and Junzhou Huang. Adaptive sampling towards fast graph representation learning. *Advances in neural information processing systems*, 31, 2018. doi:<https://dl.acm.org/doi/abs/10.5555/3327345.3327367>.
- [16] Abhinav Jangda, Sandeep Polisetty, Arjun Guha, and Marco Serafini. Accelerating graph sampling for graph machine learning using gpus. In *Proceedings of the Sixteenth European Conference on Computer Systems*, pages 311–326, 2021. doi:<https://doi.org/10.1145/3447786.3456244>.
- [17] Zhihao Jia, Sina Lin, Mingyu Gao, Matei Zaharia, and Alex Aiken. Improving the accuracy, scalability, and performance of graph neural networks with roc. *Proceedings of Machine Learning and Systems*, 2:187–198, 2020.
- [18] Bowen Jin, Chen Gao, Xiangnan He, Depeng Jin, and Yong Li. Multi-behavior recommendation with graph convolutional networks. In *Proceedings of the 43rd International ACM SIGIR Conference on Research and Development in Information Retrieval*, pages 659–668, 2020. doi:<https://doi.org/10.1145/3397271.3401072>.
- [19] Tim Kaler, Nickolas Stathas, Anne Ouyang, Alexandros-Stavros Iliopoulos, Tao Schardl, Charles E Leiserson, and Jie Chen. Accelerating training and inference of graph neural networks with fast sampling and pipelining. *Proceedings of Machine Learning and Systems*, 4:172–189, 2022.
- [20] Arpandee Khatua, Vikram Sharma Mailthody, Bhagyashree Taleka, Tengfei Ma, Xiang Song, and Wen-mei Hwu. Igb: Addressing the gaps in labeling, features, heterogeneity, and size of public graph datasets for deep learning research. In *Proceedings of the 29th ACM SIGKDD Conference on Knowledge Discovery and Data Mining*, pages 4284–4295, 2023.
- [21] Thomas N Kipf and Max Welling. Semi-supervised classification with graph convolutional networks. In *International Conference on Learning Representations*, 2016. doi:<https://doi.org/10.48550/arXiv.1609.02907>.
- [22] Marvin Klimke, Benjamin Völz, and Michael Buchholz. Cooperative behavior planning for automated driving using graph neural networks.

- In *2022 IEEE Intelligent Vehicles Symposium (IV)*, pages 167–174. IEEE, 2022. doi:<https://doi.org/10.1109/IV51971.2022.9827230>.
- [23] Adam Lerer, Ledell Wu, Jiajun Shen, Timothee Lacroix, Luca Wehrstedt, Abhijit Bose, and Alex Peysakhovich. Pytorch-biggraph: A large scale graph embedding system. *Proceedings of Machine Learning and Systems*, 1:120–131, 2019. doi:<https://doi.org/10.48550/arXiv.1903.12287>.
- [24] Jiajun Li, Ahmed Louri, Avinash Karanth, and Razvan Bunescu. Gcnax: A flexible and energy-efficient accelerator for graph convolutional neural networks. In *2021 IEEE International Symposium on High-Performance Computer Architecture (HPCA)*, pages 775–788. IEEE, 2021. doi:<https://doi.org/10.1109/HPCA51647.2021.00070>.
- [25] Zhiqi Lin, Cheng Li, Youshan Miao, Yunxin Liu, and Yinlong Xu. Pa-graph: Scaling gnn training on large graphs via computation-aware caching. In *Proceedings of the 11th ACM Symposium on Cloud Computing*, pages 401–415, 2020. doi:<https://doi.org/10.1145/3419111.3421281>.
- [26] Tianfeng Liu, Yangrui Chen, Dan Li, Chuan Wu, Yibo Zhu, Jun He, Yanghua Peng, Hongzheng Chen, Hongzhi Chen, and Chuanxiong Guo. {BGL}:{GPU-Efficient}{GNN} training by optimizing graph data {I/O} and preprocessing. In *20th USENIX Symposium on Networked Systems Design and Implementation (NSDI 23)*, pages 103–118, 2023. doi:<https://doi.org/10.48550/arXiv.2112.08541>.
- [27] Lingxiao Ma, Zhi Yang, Youshan Miao, Jilong Xue, Ming Wu, Lidong Zhou, and Yafei Dai. {NeuGraph}: Parallel deep neural network computation on large graphs. In *2019 USENIX Annual Technical Conference (USENIX ATC 19)*, pages 443–458, 2019.
- [28] Santosh Pandey, Lingda Li, Adolfo Hoisie, Xiaoye S Li, and Hang Liu. C-saw: A framework for graph sampling and random walk on gpus. In *SC20: International Conference for High Performance Computing, Networking, Storage and Analysis*, pages 1–15. IEEE, 2020. doi:<https://doi.org/10.1109/SC41405.2020.00060>.
- [29] Adam Paszke, Sam Gross, Francisco Massa, Adam Lerer, James Bradbury, Gregory Chanan, Trevor Killeen, Zeming Lin, Natalia Gimelshein, Luca Antiga, et al. Pytorch: An imperative style, high-performance deep learning library. *Advances in neural information processing systems*, 32, 2019. doi:<https://dl.acm.org/doi/10.5555/3454287.3455008>.
- [30] Bryan Perozzi, Rami Al-Rfou, and Steven Skiena. Deepwalk: Online learning of social representations. In *Proceedings of the 20th ACM SIGKDD international conference on Knowledge discovery and data mining*, pages 701–710, 2014. doi:<https://doi.org/10.1145/2623330.2623732>.
- [31] Shihui Song and Peng Jiang. Rethinking graph data placement for graph neural network training on multiple gpus. In *Proceedings of the 36th ACM International Conference on Supercomputing*, pages 1–10, 2022. doi:<https://doi.org/10.1145/3503221.3508435>.
- [32] John Thorpe, Yifan Qiao, Jonathan Eyolfson, Shen Teng, Guanzhou Hu, Zhihao Jia, Jinliang Wei, Keval Vora, Ravi Netravali, Miryung Kim, et al. Dorylus: Affordable, scalable, and accurate {GNN} training with distributed {CPU} servers and serverless threads. In *15th USENIX Symposium on Operating Systems Design and Implementation (OSDI 21)*, pages 495–514, 2021. doi:<https://doi.org/10.48550/arXiv.2105.11118>.
- [33] Petar Veličković, Guillem Cucurull, Arantxa Casanova, Adriana Romero, Pietro Liò, and Yoshua Bengio. Graph attention networks. *arXiv preprint arXiv:1710.10903*, 2017. doi:<https://doi.org/10.48550/arXiv.1710.10903>.
- [34] Petar Veličković, Guillem Cucurull, Arantxa Casanova, Adriana Romero, Pietro Liò, and Yoshua Bengio. Graph attention networks. In *International Conference on Learning Representations*, 2018. doi:<https://doi.org/10.48550/arXiv.1710.10903>.
- [35] Cheng Wan, Youjie Li, Ang Li, Nam Sung Kim, and Yingyan Lin. Bns-gcn: Efficient full-graph training of graph convolutional networks with partition-parallelism and random boundary node sampling. *Proceedings of Machine Learning and Systems*, 4:673–693, 2022. doi:<https://doi.org/10.48550/arXiv.2203.10983>.
- [36] Xinchun Wan, Kaiqiang Xu, Xudong Liao, Yilun Jin, Kai Chen, and Xin Jin. Scalable and efficient full-graph gnn training for large graphs. *Proceedings of the ACM on Management of Data*, 1(2):1–23, 2023. doi:<https://doi.org/10.1145/3589288>.
- [37] Lei Wang, Qiang Yin, Chao Tian, Jianbang Yang, Rong Chen, Wenyuan Yu, Zihang Yao, and Jingren Zhou. Flexgraph: a flexible and efficient distributed framework for gnn training. In *Proceedings of the Sixteenth European Conference on Computer Systems*, pages 67–82, 2021. doi:<https://doi.org/10.1145/3447786.3456229>.
- [38] Minjie Yu Wang. Deep graph library: Towards efficient and scalable deep learning on graphs. In *ICLR workshop on representation learning on graphs and manifolds*, 2019. doi:<https://doi.org/10.48550/arXiv.1909.01315>.
- [39] Yuke Wang, Boyuan Feng, Gushu Li, Shuangchen Li, Lei Deng, Yuan Xie, and Yufei Ding. {GNNAdvisor}: An adaptive and efficient runtime system for {GNN} acceleration on {GPUs}. In *15th USENIX symposium on operating systems design and implementation (OSDI 21)*, pages 515–531, 2021. doi:<https://doi.org/10.48550/arXiv.2006.06608>.
- [40] Xinshuo Weng, Ye Yuan, and Kris Kitani. Joint 3d tracking and forecasting with graph neural network and diversity sampling. *arXiv preprint arXiv:2003.07847*, 2(6.2):1, 2020. doi:<https://doi.org/10.48550/arXiv.2003.07847>.
- [41] Keyulu Xu, Weihua Hu, Jure Leskovec, and Stefanie Jegelka. How powerful are graph neural networks? In *International Conference on Learning Representations*, 2018. doi:<https://doi.org/10.48550/arXiv.1810.00826>.
- [42] Hongxia Yang. Aligraph: A comprehensive graph neural network platform. In *Proceedings of the 25th ACM SIGKDD international conference on knowledge discovery & data mining*, pages 3165–3166, 2019. doi:<https://doi.org/10.1145/3292500.3340404>.
- [43] Jianbang Yang, Dahai Tang, Xiaoni Song, Lei Wang, Qiang Yin, Rong Chen, Wenyuan Yu, and Jingren Zhou. Gnnlab: a factored system for sample-based gnn training over gpus. In *Proceedings of the Seventeenth European Conference on Computer Systems*, pages 417–434, 2022. doi:<https://doi.org/10.1145/3492321.3519557>.
- [44] Shuangyan Yang, Minjia Zhang, Wenqian Dong, and Dong Li. Betty: Enabling large-scale gnn training with batch-level graph partitioning. In *Proceedings of the 28th ACM International Conference on Architectural Support for Programming Languages and Operating Systems, Volume 2*, pages 103–117, 2023. doi:<https://doi.org/10.1145/32575693.3575725>.
- [45] Zuoxi Yang and Shoubin Dong. Hagerec: Hierarchical attention graph convolutional network incorporating knowledge graph for explainable recommendation. *Knowledge-Based Systems*, 204:106194, 2020. doi:<https://doi.org/10.1016/j.knosys.2020.106194>.
- [46] Rex Ying, Ruining He, Kaifeng Chen, Pong Eksombatchai, William L Hamilton, and Jure Leskovec. Graph convolutional neural networks for web-scale recommender systems. In *Proceedings of the 24th ACM SIGKDD international conference on knowledge discovery & data mining*, pages 974–983, 2018. doi:<https://doi.org/10.1145/3219819.3219890>.
- [47] Hanqing Zeng, Hongkuan Zhou, Ajitesh Srivastava, Rajgopal Kannan, and Viktor Prasanna. Graphsaint: Graph sampling based inductive learning method. In *International Conference on Learning Representations*, 2019. doi:<https://doi.org/10.48550/arXiv.1907.04931>.
- [48] Qingru Zhang, David Wipf, Quan Gan, and Le Song. A biased graph neural network sampler with near-optimal regret. *Advances in Neural Information Processing Systems*, 34:8833–8844, 2021. doi:<https://doi.org/10.48550/arXiv.2103.01089>.
- [49] Chenguang Zheng, Hongzhi Chen, Yuxuan Cheng, Zhezhen Song, Yifan Wu, Changji Li, James Cheng, Hao Yang, and Shuai Zhang. Bytengnn: efficient graph neural network training at large scale. *Proceedings of the VLDB Endowment*, 15(6):1228–1242, 2022. doi:<https://doi.org/10.14778/3514061.3514069>.

- [50] Da Zheng, Chao Ma, Minjie Wang, Jinjing Zhou, Qidong Su, Xiang Song, Quan Gan, Zheng Zhang, and George Karypis. Dist-dgl: distributed graph neural network training for billion-scale graphs. In *2020 IEEE/ACM 10th Workshop on Irregular Applications: Architectures and Algorithms (IA3)*, pages 36–44. IEEE, 2020. doi:<https://doi.org/10.1109/IA351965.2020.00011>.
- [51] Difan Zou, Ziniu Hu, Yewen Wang, Song Jiang, Yizhou Sun, and Quanquan Gu. Layer-dependent importance sampling for training deep and large graph convolutional networks. *Advances in neural information processing systems*, 32, 2019. doi:<https://dl.acm.org/doi/10.5555/3454287.3455296>.